

A Tetranuclear Hydroxo-Bridged Copper(II) Complex with Primary *N*-Acylamidines as Ligands: Preparation, Structural, and Magnetic Characterisation

Jan K. Eberhardt,^[a] Thorsten Glaser,^{*[b]} Rolf-Dieter Hoffmann,^[b] Roland Fröhlich,^[a] and Ernst-Ulrich Würthwein^{*[a]}

Keywords: *N*-Acylamidines / Copper(II) complexes / Magnetic susceptibility / N ligand / O ligand

The reaction of *N*-pivaloylbenzamidine (**1a**) and tetrakis(ace-tonitrile)copper(I) hexafluorophosphate in the presence of air yields a hydroxo-bridged copper(II) complex (**4**). The product was characterised by X-ray diffraction analysis and found to be a cubane-like dimeric complex consisting of two square dimers with the formula $[(\mathbf{1a})_2\text{Cu}_2(\text{OH})_2]_2(\text{PF}_6)_4 \cdot 4\text{CH}_2\text{Cl}_2$ (**4**·4CH₂Cl₂) with cupric ions and hydroxyl oxygen atoms at alternating vertices of a cube. The complex can be described as consisting of two [ligand-Cu-(OH)₂-Cu-ligand] units held together by long out-of-plane Cu–O bonds, creating a tetra-

meric entity with a Cu₄(OH)₄ core. Each cupric ion is essentially square-pyramidally coordinated, being bound to three OH bridges, one N atom of the amidine and one *N*-acylamidine O atom. The magnetic properties of this compound have been studied in the 2–300 K temperature range. The measurements revealed that the cupric ions in the cube are anti-ferromagnetically coupled. This observation has been rationalised on the basis of the structural data.

(© Wiley-VCH Verlag GmbH & Co. KGaA, 69451 Weinheim, Germany, 2005)

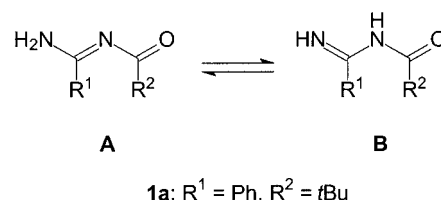
Introduction

Alkoxo-bridged Cu^{II} tetramers with cubane-like Cu₄O₄ cores are well-known. A number of complexes with this moiety have been reported and their magnetic properties have been compared with those of the corresponding binuclear compounds.^[1–7] These studies have shown that oxygen-bridged tetrameric copper(II) complexes may exhibit ferromagnetic^[8] as well as antiferromagnetic interactions. The correlation between structural parameters and magnetic properties seems to be well established.^[9]

In contrast to the alkoxy-bridged complexes, hydroxo-bridged Cu₄(OH)₄ tetramers are rather rare. To the best of our knowledge, which is based on a recent CCDC database search, only two examples have been structurally characterised, one containing bidentate 2,2'-bipyridyl ligands^[10] and the other bearing tris(2-pyridyl)amine in a bidentate coordination mode.^[11]

We report here the synthesis and solid-state molecular structure of a cubane-like hydroxo-bridged *N*-acylamidine copper(II) complex of formula $[(\mathbf{1a})_2\text{Cu}_2(\text{OH})_2]_2(\text{PF}_6)_4$ (**4**) as well as its magnetic properties measured down to 2 K.

The organic ligand employed for the synthesis of this copper complex is *N*-pivaloyl benzamidine (**1a**). *N*-Acylamidines (**1**) offer coordination sites for the formation of six membered chelates, namely the oxygen atom of the acyl functionality and the nitrogen atom of the amino group. Compounds **1** carrying an -NH₂ (primary *N*-acylamidines) or an -NHR group (secondary *N*-acylamidines) undergo tautomerism involving 1,3 proton shifts (tautomer **A** and **B**, Scheme 1).



Scheme 1. *N*-Acylamidines **1**, Tautomerism **A/B**.

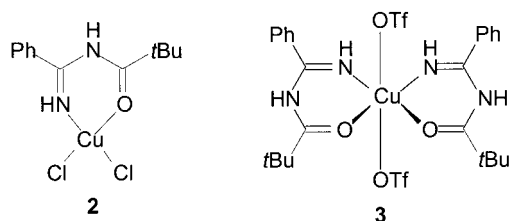
Spectroscopic data^[12] as well as crystal structure determinations^[13,14] show that the tautomer **A** dominates, while the other tautomer **B** with the two protons located on different nitrogen atoms plays, if at all, only a minor role in the equilibrium.

In earlier work we were able to characterise four monomeric copper(II) complexes with these ligands which display rather versatile coordination chemistry depending on the ligand-to-metal ion stoichiometry, the charges on the complexes and the properties of the solvents used for the syntheses (Scheme 2).^[13] For example, the reaction of *N*-piva-

[a] Organisch-Chemisches Institut der Westfälischen Wilhelms-Universität Münster, Corrensstraße 40, 48149 Münster, Germany
Fax: +49-251-83-39772
E-mail: wurthwe@uni-muenster.de

[b] Institut für Anorganische und Analytische Chemie der Westfälischen Wilhelms-Universität Münster, Wilhelm-Klemm-Straße 8, 48149 Münster, Germany
Fax: +49-251-83-33108
E-mail: tglaser@uni-muenster.de

loyl benzamidine (**1a**) with $\text{CuCl}_2 \cdot 2\text{H}_2\text{O}$ in acetonitrile and diethyl ether yielded a mononuclear 1:1 complex **2** consisting of a neutral *N*-acylamidine in its $\text{C}=\text{NH}$ tautomeric form complexed to a central copper(II) ion. The reaction of two equivalents of *N*-pivaloyl benzamidine (**1a**) with one equivalent of $\text{Cu}(\text{CF}_3\text{SO}_3)_2$ in acetonitrile and diethyl ether led to the formation of the mononuclear 2:1 copper(II) complex **3**. In complex **2** the copper(II) ion is four coordinate leading to a distorted tetrahedral structure. The 2:1 compound **3** possesses an approximate square plane around the central metal ion. Two oxygen atoms of the triflate counterions complement the coordination sphere of the copper(II) ion in axial positions.



Scheme 2. Two *N*-Pivaloyl benzamidine-Cu complexes from ref.^[13]

In another publication we presented experimental and theoretical results concerning the complexation of substituted *N*-acylamidine ligands **1** towards palladium(II), the structures of the complexes as well as their catalytic properties in cross-coupling reactions.^[15]

Results and Discussion

Synthesis

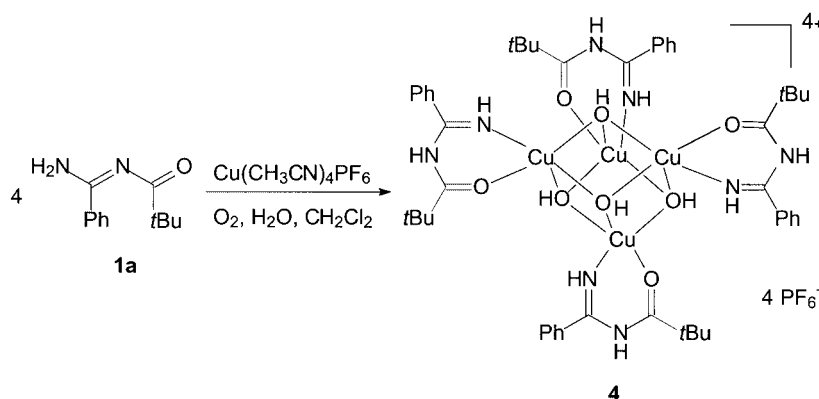
N-Acylamidines (**1**) are interesting yet rarely used ligands for metal complexation. They resemble β -dialkylamino-acroleine derivatives which have found various applications in coordination chemistry.^[16] The nitrogen atom in the 3-position of *N*-acylamidines (**1**) has a distinct influence on the electronic properties and on the reactivity of these ligands towards metal ions. A major advantage of the *N*-acylamidines (**1**) is that they are easily prepared by simple acylation of the corresponding amidines with acyl chlorides

in yields of up to 97%.^[12,17] Amidines are readily available from the reactions of nitriles with amines.^[18,19]

In a new experiment, we studied the reaction of *N*-pivaloyl benzamidine (**1a**) with copper(I) hexafluorophosphate. Equimolar amounts of **1a** and tetrakis(acetonitrile)copper(I) hexafluorophosphate were dissolved in dichloromethane, resulting in a colourless solution. A small amount of water was then added. The reaction was stirred without protection from the air leading to oxidation of the copper(I). The solution slowly turned blue due to the formation of a copper(II) complex.

Addition of an excess of diethyl ether yielded blue crystals of $[(\mathbf{1a})_2\text{Cu}^{\text{II}}(\text{OH})_2]_2(\text{PF}_6)_4 \cdot 4\text{CH}_2\text{Cl}_2$ (**4**·4CH₂Cl₂) (Scheme 3, 43% yield). The crystals lose solvent molecules indicating that the dichloromethane molecules of solvation are only weakly bound. Elemental analysis of a sample of **4**·4CH₂Cl₂ dried in air indicated the loss of one dichloromethane molecule. In a SQUID magnetometer, a high vacuum is applied to the sample to remove water and paramagnetic dioxygen. Thus, it is important to know the exact nature of the sample which is measured after the application of the high vacuum. For this purpose, it is routine to study the behaviour of samples which loose solvents of crystallization under a high vacuum before measuring such a sample in a SQUID magnetometer. Thus, a sample of **4**·4CH₂Cl₂ was dried in a high vacuum and subsequent elemental analysis indicated the presence of two molecules of dichloromethane. Detailed infrared spectroscopy indicated that no structural changes occurred in the tetranuclear complexes. Thus, the formula **4**·2CH₂Cl₂ was used for the calculation of the molecular mass and the diamagnetic correction for the analysis of the magnetic data.

The hexafluorophosphate counterion is bound to **4** via weak H-F interactions (see below). It possibly acts as a template favouring the formation of polynuclear entities. In contrast to the copper(II) chloride complex **2**, the copper ions in **4** are able to use two more coordination sites to interact with other molecules rather than with the counterions. In one of the other known examples (Sletten et al.) of a hydroxo-bridged $\text{Cu}_4(\text{OH})_4$ tetramer, hexafluorophosphate counterions were also used.^[10] In this case the hexafluorophosphate ions bridge two copper atoms within the



Scheme 3. Synthesis of **4**.

dinuclear units through loose Cu–F interactions. The tetramer reported by Marks, Ibers et al. has triflate counterions bridging two copper(II) centres.^[11]

The complexes **2** and **3** were precipitated from acetonitrile using diethyl ether. In contrast, **4** was synthesized in the less strongly coordinating solvent dichloromethane (with traces of water) and again precipitated using diethyl ether. Thus, dichloromethane offers better possibilities for interactions between metal ions and polynuclear entities are formed more easily.

From these three examples it is clear that there is a strong influence on the complex composition and molecular structure by the counterion and the solvent.

Description of the Structure

The crystal structure of $[(\mathbf{1a})_2\text{Cu}^{\text{II}}_2(\text{OH})_2]_2(\text{PF}_6)_4 \cdot 4\text{CH}_2\text{Cl}_2$ was determined by single-crystal X-ray diffraction. Figure 1 and Figure 2 show the molecular structure of the tetranuclear tetracation in crystals of $\mathbf{4} \cdot 4\text{CH}_2\text{Cl}_2$. Two dinuclear copper(II) entities are connected by long axial Cu–(OH) bonds forming a tetranuclear entity with a cubane-like $\text{Cu}_4(\text{OH})_4$ core. The Cu^{II} ions and the oxygen atoms of the hydroxy groups are located at alternating corners of a pseudo-cube.

The copper atoms are (4+1)-coordinated showing an approximate square-pyramidal geometry. One oxygen atom and one nitrogen atom from the bidentate organic ligand **1a** and two hydroxide oxygen atoms act as equatorial donors. The equatorial Cu–OH bonds are short (1.930 Å), as are the bonds to the *N*-acylamidine ligand (Cu–O 1.978 Å, Cu–N 1.935 Å). The N–Cu–O bond angles amount to 89.11°. Hence, a rhombic dimeric $\text{Cu}_2(\text{OH})_2$ entity results which interacts with a second dimer to form the observed cubane-like structure through longer axial Cu–OH bonds (2.359 Å). In the other known $\text{Cu}_4(\text{OH})_4$ cubanes, the equatorial Cu–OH distances were 1.947–1.971 Å, while the axial distances were slightly longer at 2.382–2.585 Å^[10,11] when compared with those in **4**. Within each binuclear unit, the Cu–O–Cu bridging angle is 98.84° which is similar to the values found in the literature.^[10,11] There is a slight bending within the units, the dihedral angle between the O–Cu–O planes being 6.5°.

In the $\text{Cu}_4(\text{OH})_4$ core there is one short Cu1–Cu2 separation of 2.953 Å (within the dimeric entity) and one long distance of 3.226 Å. The long separation is an interdimer copper–copper distance measured along a plane parallel to the $\bar{4}$ axis.

In compound **4**, four neutral *N*-acylamidines (**1**) in their C=NH tautomeric form **B** coordinate to one copper(II) ion each (analogous to **2** and **3**). As in the former examples (see Scheme 2), conjugated six-membered chelate rings are formed by coordination of the oxygen atoms and terminal nitrogen atoms of the *N*-acylamidines (**1**) to the metal centre. Due to the complexation, the former amino group of the ligand is transformed into an imine moiety by a formal 1,3-shift of one of the amino hydrogen atoms to the nitro-

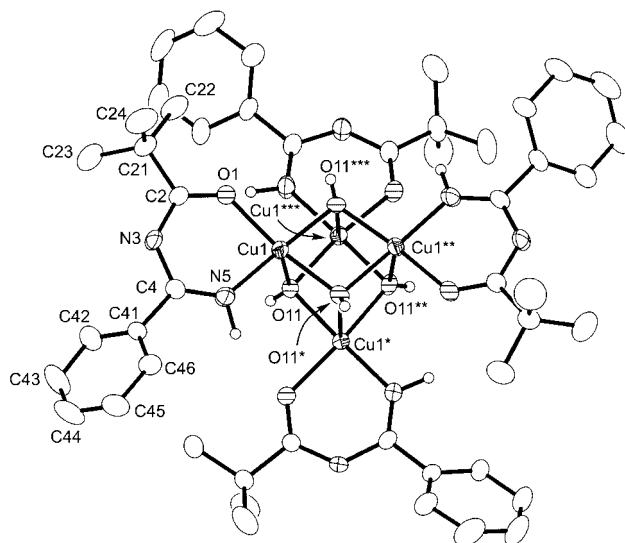


Figure 1. Molecular structure of the tetranuclear tetracation of **4** (Ortep plot) with crystallographic numbering; selected structural parameters: bond lengths [Å] Cu(1)–O(11) 1.930(3), Cu(1)–N(5) 1.935(3), Cu(1)–O(11) 1.957(3), Cu(1)–O(1) 1.978(3), Cu(1)–O(11) 2.359(3), Cu(1)–Cu(1) 2.9526(8), O(1)–C(2) 1.224(5), C(2)–N(3) 1.362(5), C(2)–C(21) 1.528(5), C(21)–C(24) 1.525(8), C(21)–C(23) 1.525(7), C(21)–C(22) 1.533(6), N(3)–C(4) 1.393(5), C(4)–N(5) 1.269(5), P(1)–F 1.558(4)–1.612(4); bond angles [°] O(11)–Cu(1)–N(5) 177.96(13), O(11)–Cu(1)–O(11) 80.79(11), N(5)–Cu(1)–O(11) 97.32(12), O(11)–Cu(1)–O(1) 92.85(11), N(5)–Cu(1)–O(1) 89.11(13), O(11)–Cu(1)–O(1) 170.98(11), O(11)–Cu(1)–O(11) 83.03(11), N(5)–Cu(1)–O(11) 96.01(15), O(11)–Cu(1)–O(11) 82.47(11), O(1)–Cu(1)–O(11) 103.22(11), O(11)–Cu(1)–Cu(1) 40.92(8), N(5)–Cu(1)–Cu(1) 137.28(10), O(11)–Cu(1)–Cu(1) 40.24(7), O(1)–Cu(1)–Cu(1) 132.47(8), O(11)–Cu(1)–Cu(1) 84.73(6), Cu(1)–O(11)–Cu(1) 98.84(11), Cu(1)–O(11)–Cu(1) 97.04(11), Cu(1)–O(11)–Cu(1) 96.29(10), C(2)–O(1)–Cu(1) 129.3(3), O(1)–C(2)–N(3) 122.4(3), O(1)–C(2)–C(21) 120.4(3), N(3)–C(2)–C(21) 17.2(3), C(24)–C(21)–C(23) 110.2(5), C(24)–C(21)–C(2) 107.2(4), C(23)–C(21)–C(2) 112.3(4), C(24)–C(21)–C(22) 109.0(5), C(23)–C(21)–C(22) 109.9(5), C(2)–C(21)–C(22) 108.3(3), C(2)–N(3)–C(4) 128.4(3), N(5)–C(4)–N(3) 121.1(3), N(5)–C(4)–C(41) 123.1(3), N(3)–C(4)–C(41) 115.8(3), C(42)–C(41)–C(46) 120.6(4), C(42)–C(41)–C(4) 121.1(4), C(46)–C(41)–C(4) 118.3(4), C(4)–N(5)–Cu(1) 129.2(3).

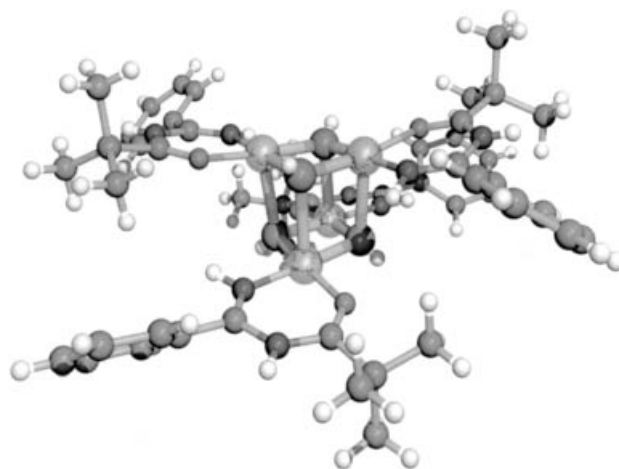


Figure 2. Povray plot of the tetranuclear tetracation of **4** (for numbering see Figure 1).

gen atom N(3). The lone pair of the sp^2 hybridised imine type nitrogen atom N(5) acts as the coordination site. Thus, the ligand **1a** presents as a conjugated $6\pi/5z$ ligand, carrying a central planar sp^2 amino group. This result is in good agreement with former experiments.^[13]

The hexafluorophosphate ions are weakly coordinated to the cationic cluster via N–H...F hydrogen bonds (2.215 Å). The H atoms of the OH groups are at a distance of 2.404 Å from the closest fluorine atom of the PF_6^- counterion, the O–H–F bond angle amounts to 146.3°.

Infrared and UV/Vis Spectra

The IR spectra of hydroxo-bridged copper(II) compounds have been studied thoroughly.^[20] The IR spectrum of **4** (KBr pellet) exhibits a characteristic doublet at 3620 and 3615 cm^{-1} which can be assigned to the bridging OH stretch in full accordance with the literature. Three sharp absorptions at 3390, 3380 and 3340 cm^{-1} can be assigned to the =NH and –NH stretching vibrations (isomer **B** of the *N*-acylamidine). In contrast, the free ligand shows bands at 3320 and 3160 cm^{-1} which can be attributed to the asymmetric and symmetric NH_2 stretching vibrations (isomer **A**), respectively.^[13] The other absorptions of the complex can be observed at common frequencies. A signal at 970 cm^{-1} has been described in the literature as a bending OH vibration.^[20] A very intense band at 845 cm^{-1} can be assigned to the stretching and bending modes of the hexafluorophosphate anions. Low intensity UV absorptions may be observed at 625 nm. These are due to d→d transitions at the metal ion which cause the blue colour of solutions of **4**.

Magnetic Susceptibility

Magnetic susceptibility data of complex **4**·2CH₂Cl₂ were measured on a microcrystalline sample in the temperature range 2–300 K with an applied field of 1 T. Note that the sample for the susceptibility measurements was dried in vacuo resulting in loss of two solvent molecules and no structural changes of **4** as demonstrated by infrared spectroscopy. A composition **4**·2CH₂Cl₂ was used for the calculation of the molecular mass and the diamagnetic correction based on elemental analysis.

Figure 3 shows the effective magnetic moment, μ_{eff} , calculated per tetranuclear unit as a function of the temperature. The temperature dependence shows a monotonic decrease from 3.60 μ_B at 300 K to 2.10 μ_B at 50 K. Below 50 K, a change in the curvature occurs. The value at 2 K is 0.66 μ_B . This behaviour is in accordance with an antiferromagnetically coupled spin-system and a total spin ground state of $S_t = 0$. The magnetic properties of the core of **4**, $[Cu^{II}_4(OH)_4]^{4+}$, were analysed with the spin Hamiltonian for four coupled spins $S_i = 1/2$ including the isotropic Heisenberg–Dirac–van Vleck (HDvV) exchange Hamiltonian and the single-ion Zeeman interaction using a full-matrix diagonalisation approach [Equation (1)].^[21]

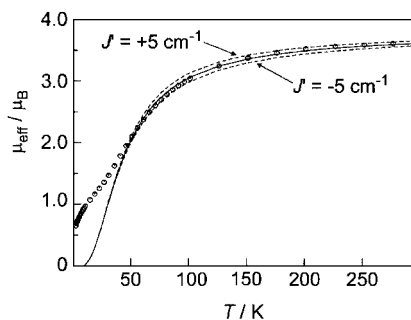


Figure 3. Temperature dependence of the effective magnetic moment, μ_{eff} , of **4**·2CH₂Cl₂ at 1 T. The solid line represents a simulation using the spin-Hamiltonian given in the text with $J = -41\text{ cm}^{-1}$, $J' = 0$, $g = 2.21$ and $\chi_{TIP} = 500 \times 10^{-6}\text{ cm}^3\text{ mol}^{-1}$. The dashed lines represent simulations using the same parameter set but using $J' = +5\text{ cm}^{-1}$ and $J' = -5\text{ cm}^{-1}$, respectively.

$$H = H_{HDvV} + \sum_{i=1}^4 \mu_B g_i S_i B \quad (1)$$

The spin topology of the $[Cu^{II}_4(OH)_4]^{4+}$ cubane is shown in Figure 4. The crystallographically imposed S_4 axes lead to the equivalence of $J = J_{13} = J_{24}$ as well as $J' = J_{12}$, J_{14} , J_{23} and J_{34} . Thus, the HDvV part of the Hamiltonian becomes [Equation (2)].

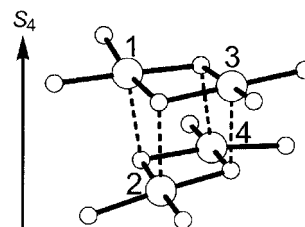


Figure 4. Spin system of **4** imposed on its molecular structure. Copper centres 1 and 3 as well as 2 and 4 both form subdimeric units. The S_4 axes yield the equivalence of the coupling constants J_{13} and J_{24} as well as the coupling constants J_{12} , J_{14} , J_{23} and J_{34} . Note that the magnetic orbitals of the Cu^{II} ions ($d_{x^2-y^2}$) are oriented in the subdimer plane perpendicular to the bond of the apical ligands.

$$H_{HDvV} = -2J(S_1S_3 + S_2S_4) - 2J'(S_1S_2 + S_1S_4 + S_2S_3 + S_3S_4) \quad (2)$$

The coupling constant J describes the interactions in the dinuclear subunits (intradimer exchange), whereas J' describes the interactions between the dimeric subunits (interdimer exchange). Dinuclear $Cu^{II}(\mu_2-OH)_2Cu^{II}$ cores are classics in magnetochemistry. A magneto-structural correlation describing the coupling constant J as a function of the Cu–O–Cu angle was established by Hodgson, Hatfield and coworkers.^[22] Applying this correlation to the dimeric subunits of complex **4** with an angle of 98.84° results in $J = -44\text{ cm}^{-1}$. The overall spin topology of the tetramer $[Cu^{II}_4(OH)_4]^{4+}$ has been found in several complexes with a

central $[\text{Cu}^{\text{II}}_4(\text{OR})_4]^{4+}$ cubane core.^[4–7,9–11] Reasonable values have been established for the intradimer coupling constants depending on the subdimer geometry. Differing magnitudes and signs have been reported for the interdimer coupling constant J' .^[4–7,9] Fallon et al. already pointed out that the interdimer interaction should be very small due to the large interdimer Cu–O distances (apical Cu–O bond of a square-pyramidal coordination geometry) when compared with the shorter intradimer Cu–O distances (equatorial Cu–O bonds of a square-pyramidal coordination geometry).^[4] They were able to fit their magnetic data only without the use of an interdimer coupling constant. Moreover, by explicitly using the appropriate tetramer model, they obtained an interdimer coupling constant of zero.^[4]

Simulation of the magnetic data of **4** using only the intradimer coupling constant J , i.e. $J' = 0$, results in a good reproduction of the experimental data above 50 K with $J = -41 \text{ cm}^{-1}$, $g = 2.21$ and $\chi_{\text{TIP}} = 500 \times 10^{-6} \text{ cm}^3 \text{ mol}^{-1}$ (solid line in Figure 3). The value of J pleasingly corroborates the value obtained from the magneto-structural correlation (vide supra). The resultant spin ladder consists of an $S_{\text{t}} = 0$ spin ground state, two $S_{\text{t}} = 1$ spin states at $+82 \text{ cm}^{-1}$, one $S_{\text{t}} = 0$, one $S_{\text{t}} = 1$ and one $S_{\text{t}} = 2$ spin state at $+164 \text{ cm}^{-1}$ (Figure 5, centre). Incorporation of an interdimer coupling constant J' does not result in a splitting of the first two excited $S_{\text{t}} = 1$ states but only in a splitting of the excited states at $+164 \text{ cm}^{-1}$. Inclusion of $J' = -5 \text{ cm}^{-1}$ splits them into $S_{\text{t}} = 0$ at $+144 \text{ cm}^{-1}$, $S_{\text{t}} = 1$ at 154 cm^{-1} and $S_{\text{t}} = 2$ at $+174 \text{ cm}^{-1}$ (Figure 5, left). On the other hand, inclusion of $J' = +5 \text{ cm}^{-1}$ splits them into $S_{\text{t}} = 2$ at $+154 \text{ cm}^{-1}$, $S_{\text{t}} = 1$ at 174 cm^{-1} and $S_{\text{t}} = 0$ at $+184 \text{ cm}^{-1}$ (Figure 5, right). These splittings do not affect the population of the spin levels at low temperatures. Thus, even taking into account an interdimer coupling, it is not possible to explain the unusual curvature of μ_{eff} below 50 K.

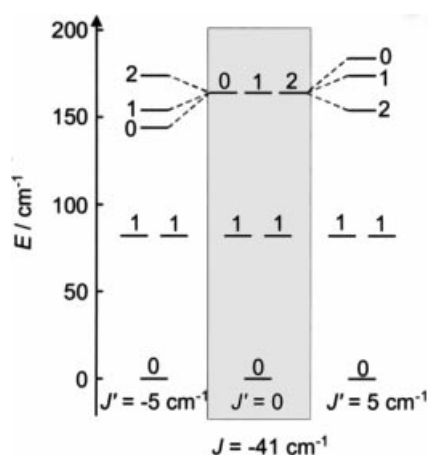


Figure 5. Spin ladder of **4** using $J = -41 \text{ cm}^{-1}$. Incorporation of $J' = -5 \text{ cm}^{-1}$ (left) or $J' = +5 \text{ cm}^{-1}$ (right) only induces a splitting of the degenerate spin states $S_{\text{t}} = 0$, 1 and 2 at 164 cm^{-1} above the spin ground state.

It seems that the deviation of μ_{eff} below 50 K originates from a paramagnetic impurity. Taking into account a para-

magnetic impurity leads to minor changes in J ($\pm 2 \text{ cm}^{-1}$) and g (± 0.02). However, this uncertainty prohibits a detailed analysis of the influence of J' . Simulations using a constant intradimer coupling constant $J = -41 \text{ cm}^{-1}$ and interdimer couplings constants $J' = +5 \text{ cm}^{-1}$ and $J' = -5 \text{ cm}^{-1}$, respectively, (dashed lines in Figure 3) indicate that the interdimer coupling should be restricted to the range $-5 \text{ cm}^{-1} < J' < +5 \text{ cm}^{-1}$. Hence, the coupling between the two dimers appears to be small.

This is in agreement with the argument of Fallon et al. whereby the interdimer distances are larger than the intradimer distances which leads to weaker superexchange pathways (vide supra).^[4] The interdimer Cu–O distances in **4** are larger (2.36 \AA) when compared with the intradimer Cu–O distances ($\approx 1.95 \text{ \AA}$). Independent of the distance point of view, the orientation of the magnetic orbitals leads to weak couplings. The magnetic orbital of each Cu^{II} ($d_{x^2-y^2}$) is oriented towards the four ligands of the dimeric subunit (Figure 4). This leads to an effective superexchange pathway across the bridging hydroxides of the subdimer. On the other hand, the magnetic orbital of each Cu^{II} ($d_{x^2-y^2}$) is of δ -type symmetry with regard to the Cu–O interaction with its apical ligand. Since these oxygen atoms do not have δ -type symmetry orbitals, there is no interaction with the magnetic orbitals of the Cu^{II} ions. Hence, the superexchange pathway through the apical ligand must be rather weak.

Conclusions

Copper(I) ions, which are important as catalysts in both enzymatic and non-enzymatic chemical systems,^[23,24,25] can be easily oxidised by molecular oxygen to Cu^{II} . Consequently, during the reaction of *N*-acylamidine **1a** with tetrakis(acetonitrile)copper(I) hexafluorophosphate in the presence of oxygen, copper(I) is transformed into copper(II) to form the tetrameric Cu^{II} complex **4** with its cubane like structure. The magnetic properties of this compound have been studied in the 2–300 K temperature range. The measurements reveal that the cupric ions in the cube are antiferromagnetically coupled.

This observation can be rationalised on the basis of the structural data. These examples clearly demonstrate that *N*-acylamidines (**1**) are very versatile ligands for copper(II) complexation. In general, they tend to form thermodynamically favourable cyclic six-membered chelates. In earlier work we found that independent of the stoichiometry used, ligand **1a** forms mononuclear 1:1 (**2**) and 2:1 (**3**) complexes with copper(II) chloride and copper(II) triflate, respectively,^[13] whereas complex **4** is formed when tetrakis(acetonitrile)copper(I) hexafluorophosphate is used. Besides the counterions, the solvent has a pronounced influence on the nature of the complexes, since the application of acetonitrile leads to complexes **2** and **3**, whereas **4** was obtained using dichloromethane.

To summarise, this series of closely related Cu^{II} complexes demonstrates well the ability of the *N*-acylamidine ligand to form structurally quite diverse copper(II) com-

plexes and underlines the intriguing role of the counterions and solvents used for the structures obtained.

Experimental Section

Materials and Methods: Compound **1a** was prepared as described previously.^[15,26] Commercially available solvents (p.a. quality) were used without further purification. The CHN analysis was performed with a Vario El III (Elementar) instrument. The melting point was measured with a differential scanning calorimeter type 910 (DuPont Instruments) with a Thermal Analyst 2000 (TA Instruments) instrument. IR spectra were recorded on a Nicolet 5DXC FTIR spectrometer as KBr pellets. UV/Vis spectra were recorded on a Cary 1 Bio spectrometer (Varian). The ¹H spectrum was obtained by using a Bruker WM 300 spectrometer.

N-Pivaloylbenzamidinocopper(II) Hexafluorophosphate Hydroxide Tetramer (4·4CH₂Cl₂): N-Pivaloylbenzamidine (**1a**, 20 mg, 0.100 mmol) was treated at room temperature with tetrakis(acetonitrile)copper(I) hexafluorophosphate (37 mg, 0.100 mmol) in dichloromethane (5.0 mL). Deionised water (0.1 mL) was then added. After stirring for 10 min, a slight precipitate was removed by filtration. Diethyl ether (7.0 mL) was carefully added to the filtrate to form an upper layer. After five days blue crystals of 4·4CH₂Cl₂ were collected. Yield: 22 mg, 0.011 mmol (43%). M.p. 171.1 °C (dec). IR (KBr): $\tilde{\nu}$ = 3620 (vs, OH), 3615 (vs, OH), 3425 (sh), 3390 (s, NH), 3380 (s, NH), 3340 (vs, NH), 3070 (w, CH_{arom.}), 2980 (s, CH_{aliph.}), 2970 (s, CH_{aliph.}), 2940 (m, CH_{aliph.}), 2920 (w, CH_{aliph.}), 2880 (w, CH_{aliph.}), 1680 (vs, C=O/C=N), 1645 (s), 1585 (w), 1555 (w), 1495 (vs), 1450 (m), 1405 (w), 1390 (m), 1375 (w), 1285 (w), 1275 (w), 1230 (m), 1190 (s), 1030 (w), 970 (w, OH), 935 (sh), 845 (vs, PF), 785 (w), 760 (s), 740 (w), 700 (s) cm⁻¹. UV/Vis (acetonitrile): λ_{max} (ϵ) = 625 (278), 247 (70367), 202 (112200) nm. ¹H NMR (300.13 MHz, CD₃CN): δ = 1.61 (m), 2.42 (m), 2.92 (br), 3.90 (m), 5.35 (br), 5.93 (s), 7.82 (br), 8.04 (br), 8.55 (m), 10.28 (br) ppm. MS (ESI, acetonitrile): m/z (%) = 616–619 (4) [C₂₄H₃₂CuF₆N₄O₂P]⁺, 470–473 (25) [C₂₄H₃₁CuN₄O₂]⁺, 236 (46) [C₂₄H₃₂CuN₄O₂]²⁺, 205 (100) [C₁₂H₁₆N₂O+H]⁺. C₄₈H₆₈Cu₄N₈O₈·4PF₆·4CH₂Cl₂ (2058.88): calcd. C 30.34, H 3.72, N 5.44; calcd. (after loss of one equivalent of dichloromethane) C 31.03, H 3.78, N 5.68; found C 31.16, H 3.84, N 5.32.

X-ray Crystal Structure Analysis for 4·4CH₂Cl₂:^[27] Formula C₄₈H₆₈Cu₄N₈O₈·4PF₆·4CH₂Cl₂, M = 2058.84, blue crystal 0.40 × 0.30 × 0.30 mm, a = 17.585(1), c = 13.726(1) Å, V = 4244.5(5) Å³, ρ_{calc} = 1.611 g cm⁻³, μ = 14.17 cm⁻¹, empirical absorption correction (0.601 ≤ T ≤ 0.676), Z = 2, tetragonal, space group $I\bar{4}$ (No. 82), λ = 0.71073 Å, T = 198 K, ω and ϕ scans, 7923 reflections collected ($\pm h$, $\pm k$, $\pm l$), $\sin \theta / \lambda$ = 0.66 Å⁻¹, 4633 independent (R_{int} = 0.032) and 4332 observed reflections [$I \geq 2\sigma(I)$], 256 refined parameters, R = 0.048, wR_2 = 0.124, max. residual electron density 0.69 (−0.66) e Å⁻³ close to the disordered CH₂Cl₂ molecules, hydrogen atoms at N3, N5 and O11 from difference Fourier calculations, others calculated and all refined as riding atoms.

Magnetic Measurements: Temperature-dependent magnetic susceptibilities of a sample of 4·4CH₂Cl₂, dried in a high vacuum, were measured in a gelatine capsule using a SQUID magnetometer (Quantum Design) at 1.0 T in the temperature range 2–300 K. This sample was analysed as 4·2CH₂Cl₂ indicating the loss of two solvated dichloromethane molecules. Infrared spectroscopic analyses before and after the drying process exhibited no changes, i.e. no structural change in the tetranuclear entity in **4** is associated with the loss of the two dichloromethane molecules. For calculations of

the molar magnetic susceptibility, χ_M , the measured susceptibilities were corrected for the susceptibilities of the sample holder and for the underlying diamagnetism of the sample using tabulated Pascal's constants and for the temperature independent paramagnetism (χ_{TIP}) which was obtained by a fitting procedure.

Acknowledgments

Financial support by the Deutsche Forschungsgemeinschaft (Sonderforschungsbereich 424) and the Fonds der Chemischen Industrie (Doktorandenstipendium for JKE) is gratefully acknowledged.

- [1] L. Walz, H. Paulus, W. Haase, H. Langhof, F. Nepveu, *J. Chem. Soc. Dalton Trans.* **1983**, 657–664.
- [2] H. Astheimer, F. Nepveu, L. Walz, W. Haase, *J. Chem. Soc. Dalton Trans.* **1985**, 315–320.
- [3] H. Oshio, Y. Saito, T. Ito, *Angew. Chem.* **1997**, 109, 2789–2791; *Angew. Chem. Int. Ed. Engl.* **1997**, 36, 2673–2675.
- [4] G. D. Fallon, B. Moubarak, K. S. Murray, A. M. van den Berg, B. O. West, *Polyhedron* **1993**, 12, 1989–2000.
- [5] L. Schwabe, W. Haase, *J. Chem. Soc. Dalton Trans.* **1985**, 1909–1913.
- [6] R. Wegner, M. Gottschaldt, H. Görls, E.-G. Jäger, D. Klemm, *Chem. Eur. J.* **2001**, 7, 2143–2157.
- [7] L. Merz, W. Haase, *J. Chem. Soc. Dalton Trans.* **1978**, 1594–1598.
- [8] N. Matsumoto, T. Kondo, M. Koder, H. Okawa, S. Kida, *Bull. Soc. Chem. Jpn.* **1989**, 62, 4041–4043.
- [9] L. Merz, W. Haase, *J. Chem. Soc. Dalton Trans.* **1980**, 875–879.
- [10] J. Sletten, A. Sørensen, M. Julve, Y. Journaux, *Inorg. Chem.* **1990**, 29, 5054–5058.
- [11] P. L. Dedert, T. Sorrell, T. J. Marks, J. A. Ibers, *Inorg. Chem.* **1982**, 21, 3506–3517.
- [12] S.-O. Chua, M. J. Cook, A. R. Katritzky, *J. Chem. Soc. Perkin Trans. 2* **1974**, 546–552.
- [13] J. K. Eberhardt, R. Fröhlich, S. Venne-Dunker, E.-U. Würthwein, *Eur. J. Inorg. Chem.* **2000**, 1739–1743.
- [14] J. Prigge, E.-U. Würthwein, unpublished results.
- [15] J. K. Eberhardt, R. Fröhlich, E.-U. Würthwein, *J. Org. Chem.* **2003**, 68, 6690–6694.
- [16] L. Kakaliou, W. J. Scanlon IV, B. Qian, S. W. Baek, M. R. Smith III, D. H. Motry, *Inorg. Chem.* **1999**, 38, 5964–5977 and references cited therein.
- [17] J. K. Eberhardt, *Diploma Thesis*, Universität Münster, **1999**.
- [18] P. Oxley, M. W. Partridge, W. F. Short, *J. Chem. Soc.* **1947**, 1110–1116.
- [19] T. Konakahara, M. Matsuki, S. Sugimoto, K. Sato, *J. Chem. Soc. Perkin Trans. 1* **1987**, 1489–1493.
- [20] J. R. Ferraro, W. R. Walker, *Inorg. Chem.* **1965**, 4, 1382–1386 and references cited therein.
- [21] The routine JULIUS was used for spin Hamiltonian simulations of the data (C. Krebs, F. Birkelbach, V. Staemmler, E. Bill, unpublished results).
- [22] V. H. Crawford, H. W. Richardson, J. R. Wasson, D. J. Hodgson, W. E. Hatfield, *Inorg. Chem.* **1976**, 15, 2107–2110.
- [23] R. H. Holm, P. Kennepohl, E. I. Solomon, *Chem. Rev.* **1996**, 96, 2239–2314.
- [24] N. Oishi, Y. Nishida, K. Ida, S. Kida, *Bull. Chem. Soc. Jpn.* **1980**, 53, 2847–2850.
- [25] *Modern Organocopper Chemistry* (Ed.: N. Krause), Wiley-VCH, Weinheim, **2002**.
- [26] M. Buhmann, *Diploma Thesis*, Universität Münster, **1989**.
- [27] Data set was collected with a Nonius KappaCCD diffractometer, equipped with a rotating anode generator. Programs used: data collection COLLECT (Nonius B.V., 1998), data reduction Denzo-SMN [a] Z. Otwinowski, W. Minor, *Methods in Enzymology* **1997**, 276, 307–326], absorption cor-

rection SORTAV [b] R. H. Blessing, *Acta Crystallogr. Sect. A* **1995**, *51*, 33–37; c) R. H. Blessing, *J. Appl. Crystallogr.* **1997**, *30*, 421–426], structure solution SHELXS-97 [d] G. M. Sheldrick, *Acta Crystallogr. Sect. A* **1990**, *46*, 467–473], structure refinement SHELXL-97 [e] G. M. Sheldrick, University of Göttingen, **1997**].

[28] CCDC-249168 contains the supplementary crystallographic data for this paper. These data can be obtained free of charge from The Cambridge Crystallographic Data Centre via www.ccdc.cam.ac.uk/data_request/cif.

Received: September 21, 2005